JOURNAL OF AGRICULTURAL AND FOOD CHEMISTRY
ARTICLE

J. Agric. Food Chem. 2010, 58, 8895–8903 8895
DOI:10.1021/jf101778t

A Fluoroimmunoassay Based on Quantum Dot−Streptavidin Conjugate for the Detection of Chlorpyrifos

Yiping Chen,[†] He ling Ren,[†] Nan Liu,[‡] Na Sai,[§] Xiaoyu Liu,[†] Zhen Liu,[†] Zhixian Gao,*[,†,‡] and Bao an Ning*[,‡]

[†]College of Food Science and Technology, Huazhong Agricultural University, Wuhan, 430070, China, [‡]Tianjin Key Laboratory of Risk Assessment and Control Technology for Environment & Food Safety, Institute of Hygiene and Environmental Medicine, Tianjin, 300050, China, and [§]School of Chemical Engineering and Technology, Tian Jin University, Tianjin, 300072, China

A rapid and sensitive competitive fluorescence-linked immunosorbent assay (cFLISA) based on quantum dot−streptavidin conjugate (QDs−SA) was developed for the detection of chlorpyrifos in drinking water. The QDs−SA conjugate, which consists of 3-mercaptopropyl acid-stabilized CdTe nanoparticle QDs and streptavidin (SA) made through the active ester method, was employed to improve the sensitivity of QDs−SA-cFLISA. The 50% inhibition concentration (IC_{50}) and the limit of detection (LOD) were 28.5 and 3.8 ng mL^{-1}, respectively. QDs−SA-cFLISA increased sensitivity 5.5-fold and reduced detection time by 1 h compared with conventional enzyme-linked immunosorbent assay (ELISA). With chlorpyrifos concentrations of 100, 50, and 20 ng mL^{-1}, recoveries ranged from 85.9% to 105.3% with coefficients of variation ranging from 6.3% to 13.5%. This study demonstrated that QDs−SA-cFLISA was more rapid and sensitive than conventional ELISA. Therefore, it can be used as a novel screening method for the detection of pesticide residues.

KEYWORDS: Quantum dot−streptavidin; fluoroimmunoassay; chlorpyrifos

INTRODUCTION

The issue regarding the presence of pesticide residues in food and the environment has attracted extensive public attention in recent years (*1*). Serious environmental and health problems are arising due to the widespread use and abuse of pesticides (*2*). Thus, it has become increasingly important to detect and monitor the level of pesticide residues in food and the environment. At present, the identification and quantification of pesticides are generally based on chromatographic methods, such as gas chromatography (GC) and high-performance liquid chromatography coupled with mass spectroscopy (HPLC−MS)(*3*). Although these methods are sensitive and reliable, they are time-consuming and highly costly. Moreover, they can only be performed by well-trained technicians and are not convenient for on-site or in-field detection. Therefore, rapid and sensitive assays should be developed for detecting pesticide residues in food and the environment. With the development of nanotechnology, obtaining a new class of highly fluorescent homogeneous semiconductor nanocrystals called "quantum dot" has become possible (*4*).

QDs, such as CdSe−ZnS core shell nanocrystals, are somewhat spherical nanocrystals with diameters ranging from 1 to 10 nm (*5*). These comprise a series of luminescent inorganic fluorophores with several important advantages over traditional fluorescent dyes (*6*). For example, QDs have long-term photostability, high quantum yield, narrow emission and broad excitation spectra, making it possible to excite a number of different QDs using a single excitation laser wavelength. Moreover, the emission color of QDs is tunable by changing the nanocrystal size and the type of core material used, hence, simultaneous multianalyte detection can be achieved easily using multicolor QDs. Recently, QDs have been successfully used for a variety of bioanalytical purposes, such as biosensing (*7*), DNA hybridization detection (*8*), cellular labeling (*9*), biological imaging (*10*) and immunoassays. Direct, sandwich and competitive assays have likewise been developed to detect protein toxins and veterinary drug residues such as staphylococcal enterotoxin B (SEB) (*11*), trinitrotoluene (TNT) (*12*), sulfamethazine and enrofloxacin residue (*13*−*15*)).

Over the past decade, enzyme-linked immunosorbent assay (ELISA) has become an important alternative detection method for pesticides, particularly in analyzing a large number of samples. It is also being used as a screening tool, because of its numerous practical benefits, including cost efficiency, consistency, portability, and ease of use (*16*).

QDs, as relatively new fluorescent probes, have particularly played an important role in fluoroimmunoassay (*17*). At the same time, the biotin−streptavidin system (B−S system), a signal amplification system, has been widely used in immunohistochemistry (*18*) and immunoassays (*19*) for its high specificity and strong affinity. Streptavidin (SA) contains four binding sites with an extraordinary affinity (dissociation constant: about 10^{-15} M) for the capture of the small molecule biotin which can be easily covalently coupled to proteins to enable a solid binding between those proteins and SA.

Chlorpyrifos, a kind of phosphate pesticide and environmental endocrine disruptor, has been widely used in agriculture to kill

*Corresponding authors. Z.G.: phone, +86-022-84655191; fax, +86-022-84655191; e-mail, gaozhx@163.com. B.a.N.: phone, +86-022-84655403; fax, +86-022-84655191; e-mail, ningba@163.com.

Published on Web 07/27/2010

pests. Its residue is found mainly in farm soil and environmental water (*20*). Nowadays, numerous facts suggest that residual chlorpyrifos poses a possible risk to the environment and human health (*21*). Its presence in drinking water, specifically, is harmful to humans. Thus, the Environmental Protection Agency (EPA) Method 525 has set the maximum allowable risk level for organophosphorus pesticides (OPs) in drinking water within the range of 0.001 to 0.25 mg mL^{-1}. Conventional analytical methods for the detection of chlorpyrifos in environmental water samples include gas chromatographic−mass spectrometric (GC−MS) and HPLC, both of which are costly and time-intensive (*22*). Therefore, it is necessary to develop a rapid, simple and sensitive method to monitor residual chlorpyrifos in drinking water.

In this study, a rapid and sensitive fluoroimmunoassay (QDs−SA-cFLISA) based on QDs−SA conjugate was developed for the detection of chlorpyrifos in drinking water. To our knowledge, this is the first study focused on the analysis of chlorpyrifos residue using QDs and the B−S system. In this assay, QDs−SA conjugate was used as a fluorescence signal system and a signal amplification system to improve test sensitivity, conventional ELISA and HPLC methods were employed for methodology comparison.

MATERIALS AND METHODS

Reagents. Chlorpyrifos and its analogues and intermediates were purchased from Sigma Chemical Co (St. Louis, MO). The monoclonal antibody against chlorpyrifos (Ab_1) was purchased from Wanghua Biotechnology (Beijing, China). SA was purchased in Biosynthesis Biotechnologyco. (Beijing, China). *N*-Hydroxysulfosuccinimide sodium salt (sulfo-NHS), 1-ethyl-3-(3-dimethylaminopropyl)carbodiimide (EDC) and 3-mercaptopropyl acid (MPA) were purchased from Sigma. Tellurium powder (200 mesh, 99.8%), $CdCl_2$ (99%) and $NaBH_4$ (99%) were purchased from Aldrich. In order to determine quantum yields of QDs, rhodamine 6G with a quantum yield of 95% in ethanol was obtained from Sinopharm chemical Reagent Beijing Co. Ltd. (Beijing, China). Common solvents and salts were supplied by Tianjin Regent Corp. (Tianjin, China). The coating buffer used was 0.05 mol L^{-1} carbonate buffer (pH 9.6), washing buffer was 0.01 mol L^{-1} phosphate-buffered saline (PBS) with 0.05% Tween 20 (PBST) (pH 7.4) and blocking buffer was PBS buffer with 3% skim milk power. Chlorpyrifos and its analogues were prepared by dissolving known amounts of purified substances in methanol. The stock solution (10 mg mL^{-1}) was stored at −20 °C before being used for the preparation of standard solutions, which were stored at 4 °C. Pure water was prepared using the Milli-Q system from Millipore (Bedford, MA).

Apparatus. Costar opaque black polystyrene microtiter plates were purchased from Corning, Inc. (New York). The 96-well ELISA microtiter plates were obtained from Wanger Biotech Co (Beijing, China). Ultrafiltration units (15 mL, 4 and 0.5 mL) and 0.2 μm PES membrane units were also purchased from Millipore. Biotinylated monoclonal antibody (Biotinylated-Ab_1) was separated and purified using YM-10 columns (MWCO, 10,000; pack size, 8; Millipore, USA). Cary Eclipse fluorescence spectrophotometer (Palo Alto, CA) and a SpectraFluor Plus microtiter plate reader (Massachusetts) were used to obtain the fluorescence signal. A protein electrophoresis apparatus from Bio-Rad. Inc. (California) was used to characterize the complete antigen (chlorpyrifos−BSA conjugate). A centrifuge, Mikro 22R from Hettich Co. (Kirchlengern, Germany) and HPLC system (Waters, USA) were also used in the study.

Synthesis of Water-Soluble CdTe QDs. QDs were synthesized in an aqueous solution according to a previous report (*23*). In brief, freshly prepared oxygen-free NaHTe solution was added to a nitrogen saturated 1.25×10^{-3} mol L^{-1} $CdCl_2$ aqueous solution (pH = 11.4) in the presence of MPA as stabilizing agent. NaHTe was prepared by the reaction of $NaBH_4$ with tellurium powder at a 2:1 molar ratio. The molar ratio of Cd^{2+} to MPA to Te^{-} was 1:2.4:0.5. The solution was refluxed for different time periods to control the size of the QDs.

The obtained QDs solution was further purified via ultrafiltration according to a previous report (*24*). The first step was carried out on a filter with a size of 10,000 MW, after which the solution was centrifuged at 4000 rpm (10 min, 4 °C) to remove nonreacted MPA. The QDs were washed three times with 50 mmol L^{-1} PBS (pH 7.4). The upper phase was collected, dissolved in PBS, and subjected to a second ultrafiltration step through a 50,000 MW filter. After the second ultrafiltration step, the lower and upper phases were collected for the next stage of the experiment. The purified water-soluble QDs were characterized by bright fluorescence and good stability in PBS buffer.

Optical Characterization of the CdTe QDs. Fluorescence spectra of the QDs was taken using a Cary Eclipse fluorescence spectrophotometer equipped with a 20 kW xenon discharge lamp as a light source. Spectra were typically taken at a scanning rate of 1000 nm/min with 10 nm excitation/emission slits and a 700 V photomultiplier tube voltage. The dispersion and sizes of CdTe QDs were evaluated with a transmission electron microscopy (TEM).

Quantum Yield (QY) of the CdTe QDs. QY was calculated according to a previous report (*25*). Rhodamine 6G was used as the fluorescence standard to measure the fluorescence QY of the CdTe QDs. Specifically, rhodamine 6G was dissolved in anhydrous alcohol with an absorbance rate of around 0.02 and the normal excitation wavelength of 470 nm. By comparing the integrated areas of emissions from rhodamin 6G and QDs, respectively, the fluorescence QY values of QDs were calculated by taking rhodamine 6G in diluted solution.

Formation and Purification of the QDs−SA Conjugate. The conjugate of CdTe QDs with SA was prepared through the active ester method described in a previous work with some modifications (*26*). The 200 μL 10 μM QDs solution produced through purification was mixed with 200 μL of SA solution in PBS (0.01 mol L^{-1}, pH 7.4), and the molar ratio of QDs/SA was optimized. Thereafter, 20 μL of freshly prepared 10 mg mL^{-1} EDC solution and 30 μL of freshly prepared 10 mg mL^{-1} sulfo-NHS solution were added to the mixture quickly. The samples were incubated for 2 h at room temperature (RT) under continuous shaking in the dark. The conjugate solution was filtered through a 0.2 μm PES membrane unit to remove the protein conjugates; this was transferred to a clean centrifugal ultrafiltration unit (a 50,000 MW filter), where it was centrifuged at 8000 rpm for 15 min at 4 °C. The free nonconjugated SA, as well as the isourea byproduct of the conjugation reaction, was removed by ultrafiltration. The upper phase, which contained the QDs−SA conjugate, was decanted and diluted into 2.0 mL of PBS, after which 0.5 mL of 50 mmol L^{-1} PBS with 0.5% bovine serum albumin (BSA) was then added. The QDs−SA conjugate solution (8 mM) was stored at 4 °C.

Preparation of the Chlorpyrifos−BSA Conjugate (Ag). The chlorpyrifos−BSA conjugate was produced according to a previous report with some modifications (*27*). The synthesis pathway of the chlorpyrifos−BSA conjugate is shown in **Figure 1**. First, a chlorpyrifos−propionic acid derivative was synthesized through the reaction between chlorpyrifos and 3-mercaptopropyl acid (**Figure 1a**). Second, the derivative was coupled with BSA by the carbodiimide method using EDC and sulfo-NHS (**Figure 1b**). After conjugation, the mixture was transferred to a clean centrifugal ultrafiltration unit (a 10,000 MW filter) and centrifuged at 8000 rpm (15 min at 4 °C). Unreacted hapten (chlorpyrifos) and the byproduct were removed by ultrafiltration. The conjugate was then characterized by sodium dodecyl sulfate−polyacrylamide gel electrophoresis (SDS−PAGE), and was freeze-dried and stored at −20 °C.

Formation and Purification of the Biotinylated-Ab_1 Conjugate. NHS-LC-Biotin was diluted to 1 mg mL^{-1} by DMF and Ab_1 was diluted to 1 mg mL^{-1} by 0.1 g L^{-1} $NaHCO_3$, (pH 9.6). The two solutions were mixed at a 10:1 ratio by volume (NHS-LC-Biotin/Ab_1) and stirred for 3 to 4 h for the biotinylation of Ab_1. After labeling, the mixed solution was transferred to a YM-10 column and centrifuged at 10,000 rpm (15 min, 4 °C). Excessive unreacted biotin and ions in the aqueous solution were removed by YM-10 column, and the biotin-labeled Ab_1 was eluted with 10 mmol L^{-1} PBS (pH 7.2). It was then aliquoted and stored at −20 °C until use.

The QDs−SA-cFLISA Method. The schematic diagram of the QDs−SA-cFLISA procedure is shown in **Figure 2**. A 96-well opaque black microtiter plate was coated with 100 μL/well of the coating antigen (chlorpyrifos−BSA), diluted with coating buffer (0.05 mol L^{-1} $NaHCO_3$, pH 9.6) and incubated at 37 °C for 2 h. The unbound antigen was washed four times with 0.05% Tween-20 in a phosphate buffer solution (PBST), and the excess binding sites were blocked by 150 μL/well of 3% skim milk power in PBS at 37 °C for 1 h. Subsequently, 50 μL of the samples (drinking water sample or standard serial dilutions of chlorpyrifos in PBS), together with 50 μL of the optimal biotinylated-Ab_1 dilution, was added to

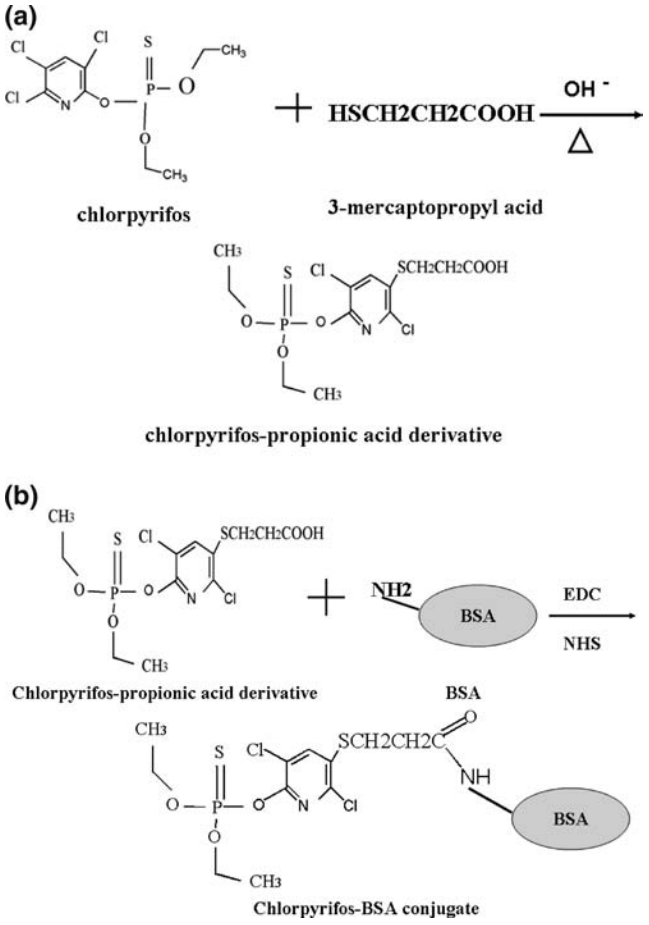

Figure 1. (**a**) The schematic diagram of the chlorpyrifos−propionic acid derivative synthesis. (**b**) The schematic diagram of the chlorpyrifos−BSA conjugate synthesis.

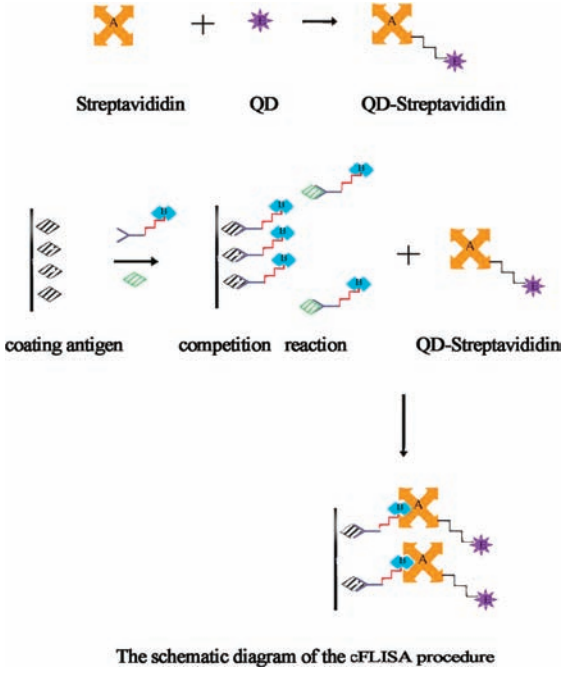

Figure 2. The schematic diagram of the QDs−SA-cFLISA method procedure.

the wells (in triplicate). The plate was then incubated for 1.5 h at 37 °C. After washing five times, the 100 μL/well QDs−SA conjugate was added to the wells and incubated for 0.5 h at 37 °C. After incubation, the plate was washed seven times and patted dry. A fluorescence microplate reader with an excitation/emission at 300/600 nm was utilized to measure the fluorescence signal. A four-parameter logistic equation was used to fit the QDs−SA-cFLISA data. Calculations were performed with OriginPro7.5 software. The IC_{50} and LOD served as criteria to evaluate the QDs−SA-cFLISA; these different characteristics represented the analyte concentrations obtained at 50% and 10%, respectively.

The Conventional ELISA Method. The procedure before adding the QDs−SA conjugate was the same as that for QDs−SA-cFLISA. After washing five times with PBST, 100 μL/well goat polyclonal antibody to mouse IgG-HRP (1:4000) was added and incubated for 1 h at 37 °C, and the plate was then washed seven times. Subsequently, 100 μL of tetramethylbenzidine substrate system was added into the well and incubated for 15 min at 37 °C in the dark. The enzymatic reaction was then quenched by adding 50 μL/well of 2 mol L^{-1} H_2SO_4. The absorbance was measured with an ELISA microplate reader at 450 nm, and the chlorpyrifos content in unknown samples was calculated based on the calibration curve, which was generated during the same run.

Cross-Reactivity (CR). In our research, the CR of the compounds structurally related to chlorpyrifos was investigated with the Ab_1 by QDs−SA-cFLISA and conventional ELISA. The CR values were calculated according to eq 1.

$$\mathrm{CR}\ (\%) = \frac{IC_{50}\ \text{of chlorpyrifos}}{IC_{50}\ \text{of chlorpyrifos analogues}} \times 100 \qquad (1)$$

Optimal Concentration of Biotinylated-Ab_1 and Ag in ELISA. At first, optimum concentration of biotinylated-Ab_1 and Ag was selected by checkerboard titration in ELISA. At the base of checkerboard titration, different concentrations of biotinylated-Ab_1 (30, 20, 15 ng mL^{-1}) and Ag (0.30, 0.20, 0.15 μg mL^{-1}) were observed during the competitive step in ELISA.

Optimization of the Molar Ratio of QDs/SA. 100 μL/well QDs−SA conjugate solutions with different QDs/SA ratios (2:1, 1:1, 1:2 and 1:3) were tested using QDs−SA-cFLISA under the optimized concentrations of biotinylated-Ab_1 and Ag, respectively.

Effect of pH on the Coupled Reaction of QDs and SA. A series of pH gradients (5.5, 6.0, 6.5, 7.0, 7.5 and 8.0) were set in order to observe the effect on the QDs and SA coupling reaction. The resulting conjugates were tested by QDs−SA-cFLISA.

Optimized Dilution Level of the QDs−SA Conjugate. 100 μL/well serial dilutions of the QDs−SA conjugate solution (1:10, 1:20, 1:50) were observed to select the optimal level of the QDs−SA conjugate by QDs−SA-cFLISA.

The HPLC Method. The procedures of extraction and cleanup of samples were carried out according to the Chinese national standard (GB 19605-2004) with modifications. Briefly, a 250 mL water sample was purified by a C_{18} SPE column, and the adsorbate was eluted by 3 mL of mobile phase. The extractive sample was prepared for analysis. The optimized chromatographic conditions were as follows: column, C_{18} (250 × 4.6 mm, 5 μm); injection volume, 50 μL; mobile phase, acetonitrile−water−acetic acid (82:17.5:0.5 v/v/v); flow rate, 1.0 mL min^{-1} at RT; detection wavelength, 265 nm.

Matrix Effect. Drinking water, surface water and agricultural runoff water were collected from water works, Jingye Lake and the Haihe River in Tianjin, respectively. Water samples were centrifuged at 5000 rpm (5 min) to remove suspended particles and then stored at 4 °C. For this study, chlorpyrifos standard curves were prepared in PBS, drinking water, agricultural runoff waters and surface water matrix, each fortified at eight concentrations (500, 200, 100, 50, 25, 12.5, 6.25, 1 ng mL^{-1}) and analyzed in triplicate. The matrix effect was assessed through the comparison of competitive inhibition curves with the standard curve in PBS buffer.

Accuracy and Precision Analysis. First, different volumes of chlorpyrifos standard stock solution (1 mg mL^{-1}) were added into the PBS buffer to produce samples with a series of chlorpyrifos concentrations (100, 50 and 20 ng mL^{-1}); the tubes were shaken at RT for 5 min and stored at 4 °C for conventional ELISA and QDs−SA-cFLISA analyses.

Drinking Water for Analysis. The quality of drinking water is directly related to human health. Thus, drinking water was selected as a prior object in our study. At first, the sample was diluted at a series of ratios (1:1, 1:2 and 1:4) by PBS buffer (0.01 M, pH 7.4) to minimize the

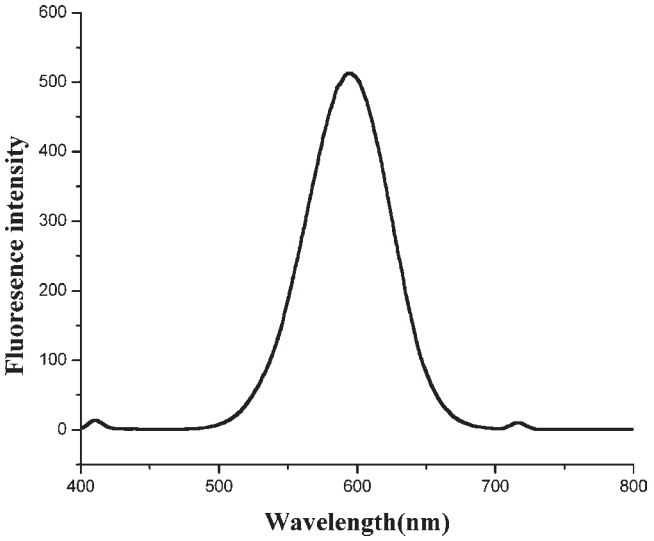

Figure 3. Emission spectra of red QDs; the emission peak is at 595 nm with full width at half-maximum of 55 nm.

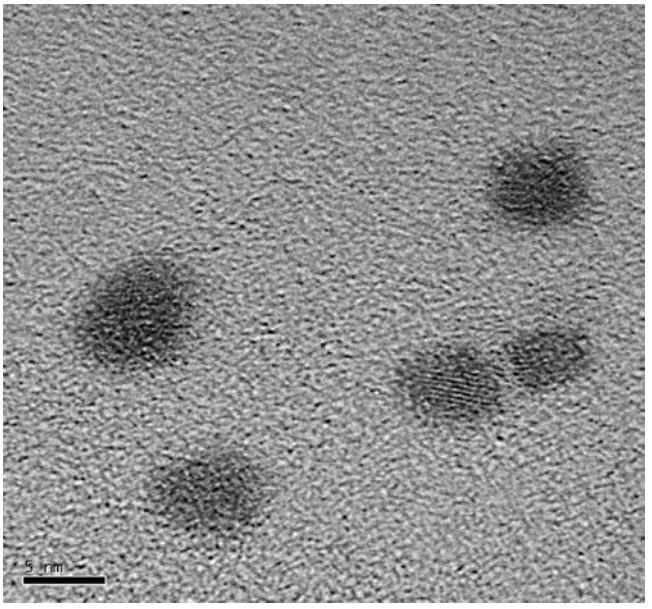

Figure 4. The dispersion and sizes of CdTe QDs were evaluated by a transmission electron microscopy (TEM), and the measuring scale in the image is 5 nm.

complex matrix effect, which was assessed through the comparison of competitive inhibition curves with the standard curve in PBS buffer. The diluted water was then prepared for the HPLC, ELISA and QDs−SA-cFLISA detection procedures.

RESULTS AND DISCUSSION

Fluorescent Features of QDs. A fluorescence spectrum of QDs is shown in **Figure 3**. The emission spectral bandwidth is narrow and symmetric (with a full width at a half-maximum of about 55 nm). Simultaneously, the excitation spectrum was broad. Unlike organic dyes, these optical qualities can minimize channel overlap, improve color discrimination, and enable multiplexing without compensation or the use of multiple excitation filters.

The dispersion and the size of CdTe QDs were evaluated via TEM. The carboxylic group-modified QDs were well dispersed, and the size of the QDs was about 6 nm (**Figure 4**). Homogenicity is an important parameter for evaluating the quality of QDs.

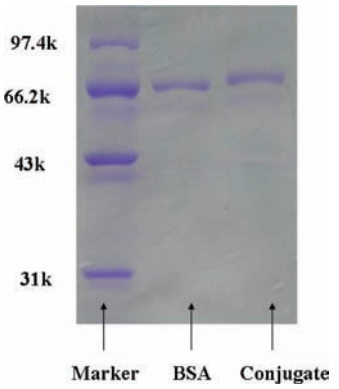

Figure 5. SDS−PAGE of chlorpyrifos−BSA conjugate and BSA.

Well-dispersive QDs can greatly eliminate aggregation and extend the application of QDs in different fields.

The QY of QDs was also a key factor in judging the performance of QDs. In our study, the QY of the red CdTe QDs was 28.9%. As a water-soluble QDs, it has a high QY compared to congeneric QDs.

Chlorpyrifos−BSA Conjugate Verification. SDS−PAGE electrophoresis was used as a simple and direct visual method for observing the conjugation. In the study, 12% separation gel was used; the markers were low molecular weight (MW) proteins with sizes ranging from 14 kD to 97 kD. BSA moved further than the chlorpyrifos−BSA conjugate because the MW of BSA was smaller than that of the conjugate, suggesting that the conjugate was successfully prepared (**Figure 5**).

Method Optimization. The sensitivity of QDs−SA-cFLISA depends on both the method itself and a series of experimental parameters. The concentrations of biotinylated Ab_1 and Ag, the molar ratio of QDs/SA, the dilution level of the QDs−SA conjugate, the pH of reaction system and nonspecific absorption served as the main factors influencing the sensitivity of QDs−SA-cFLISA.

The Optimal Concentration of Biotinylated Ab_1 and Ag. The concentration of Ag and Ab_1 is a key factor influencing the sensitivity of an immunoassay. Thus, Ab_1 (20 ng mL^{-1}) and Ag (200 ng mL^{-1}) were selected in the next step (**Figures 6a** and **6b**).

The Molar Ratio of QDs/SA. Quantitation of the number of molecules bound per QDs has attracted the attention of many researchers. Goldman (*28*) found the ideal QDs/antibody ratio to be 1:1. In this study, the result (**Figure 7a**) showed that the relative fluorescence intensity was the largest when the ratio of QDs/SA was 1:3; however, this conjugate was not stable and often aggregated in a few days. On the other hand, the 1:2 ratio of the conjugate was more stable than the 1:3 ratio; hence, the 1:2 ratio of the conjugate was selected for the next experiment. The reason might be that the carboxyl group on the surface of 3-mercaptopropyl acid-stabilized CdTe QDs not only behaved as a reactive group but also served as the stable agent responsible for preventing QDs aggregation through electrostatic repulsion. If the carboxy group has been mainly reacted in the labeling procedure, the QDs may be aggregated due to missing electrostatic repulsion.

Optimized pH in the Coupling Reaction of QDs and SA. The surface charges of QDs and SA that affect their stability can be adjusted by changing the pH of the reaction system. Moreover, pH is related to the reactivity of EDC and NHS. EDC-mediated amide bond formation effectively occurs between pH levels of 4.5 and 7.5. Beyond this range, the coupling reaction occurs more slowly, resulting in lower yields. The most effective pH for the reactivity of NHS is about 8.0 (*29*). In this study, pH 7.0 was selected for the coupling reaction between QDs and SA (**Figure 7 b**).

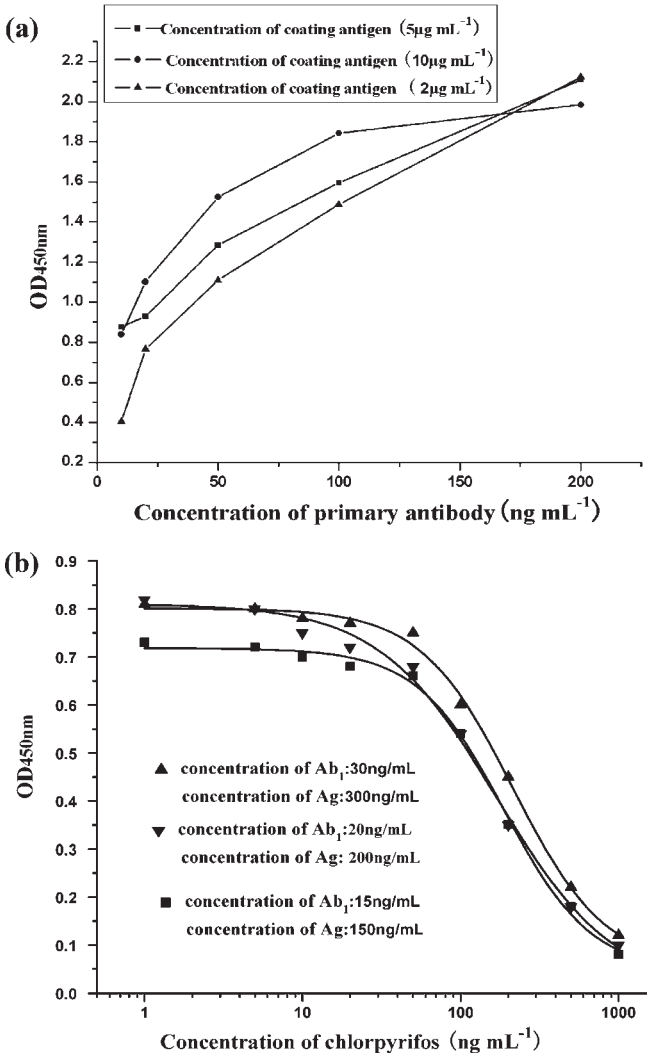

Figure 6. Optimized concentration of biotinylated-Ab_1 and Ag in ELISA. (**a**) Concentration of biotinylated-Ab_1 and Ag was first observed by checkerboard titration. When OD_{450nm} = 1, the concentration of biotinylated-Ab_1 and Ag was selected for the next step. (**b**) Effect of concentration of biotinylated-Ab_1 and Ag in the sensitivity.

Optimal Dilution Ratio of the QDs−SA Conjugate. The binding of QDs to Ab_1 occurs through the interaction between SA and biotin. Hence, the relative molar ratio of the QDs−SA conjugate to biotinylated-Ab_1 is important. Based on the optimized concentration of biotinylated-Ab_1 and Ag, QDs−SA-cFLISA was the most sensitive when QDs−SA conjugate was diluted 20-fold and the final concentration was 0.4 mM (**Figure 7c**).

Sensitivity. In the above optimal conditions, the sensitivity levels of conventional ELISA and QDs−SA-cFLISA were investigated using the chlorpyrifos standard.

For conventional ELISA, the standard curves (**Figure 8a**) were obtained under optimal Ag (200 ng mL^{-1}), Ab_1 (20 ng mL^{-1}) and Ab_2 concentration (1:4000). The IC_{50} and LOD for chlorpyrifos were 96.8 ng mL^{-1} and 20.6 ng mL^{-1}, respectively.

For QDs−SA-cFLISA, the standard curves (**Figure 8b**) were obtained under optimal Ag (200 ng mL^{-1}), biotinylated-Ab_1 (20 ng mL^{-1}), and QDs−SA (0.4 mM). The IC_{50} and LOD for chlorpyrifos were 28.5 ng mL^{-1} and 3.8 ng mL^{-1}, respectively. The sensitivity increased 5.5-fold compared with conventional ELISA; hence, it can meet current EPA and WHO standards for the detection of chlorpyrifos in drinking water. For further research, a higher bioactive and qualitative QDs−SA conjugate should be prepared and applied in QDs−SA-cFLISA immunoassay to detect pesticide residues in environment and food.

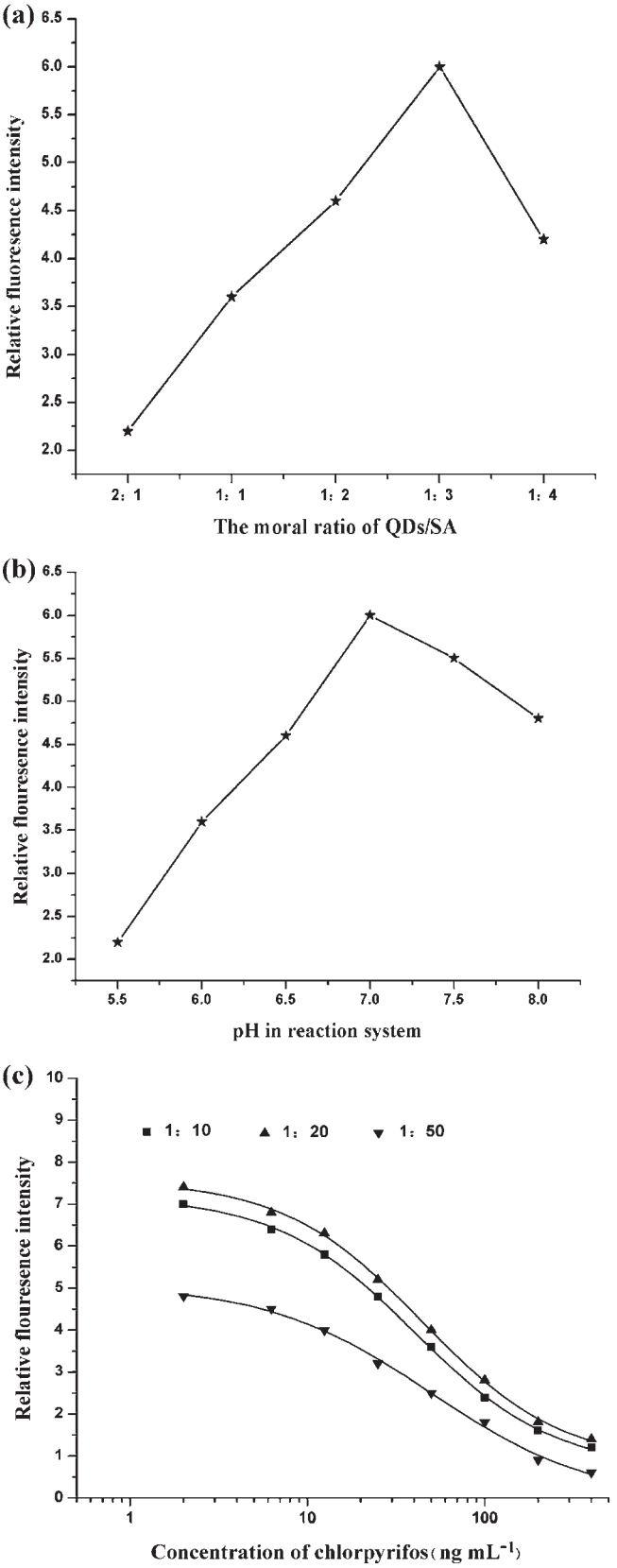

Figure 7. (**a**) Optimize the molar ratio of QDs/SA in QDs−SA conjugate. (**b**) Effect of pH in formation of QDs−SA conjugate. (**c**) Optimize dilution level of QDs−SA conjugate. Three dilution levels QDs−SA conjugate (1:10, 1:20 and 1:50) were observed to obtain optimal sensitivity of QDs−SA-cFLISA.

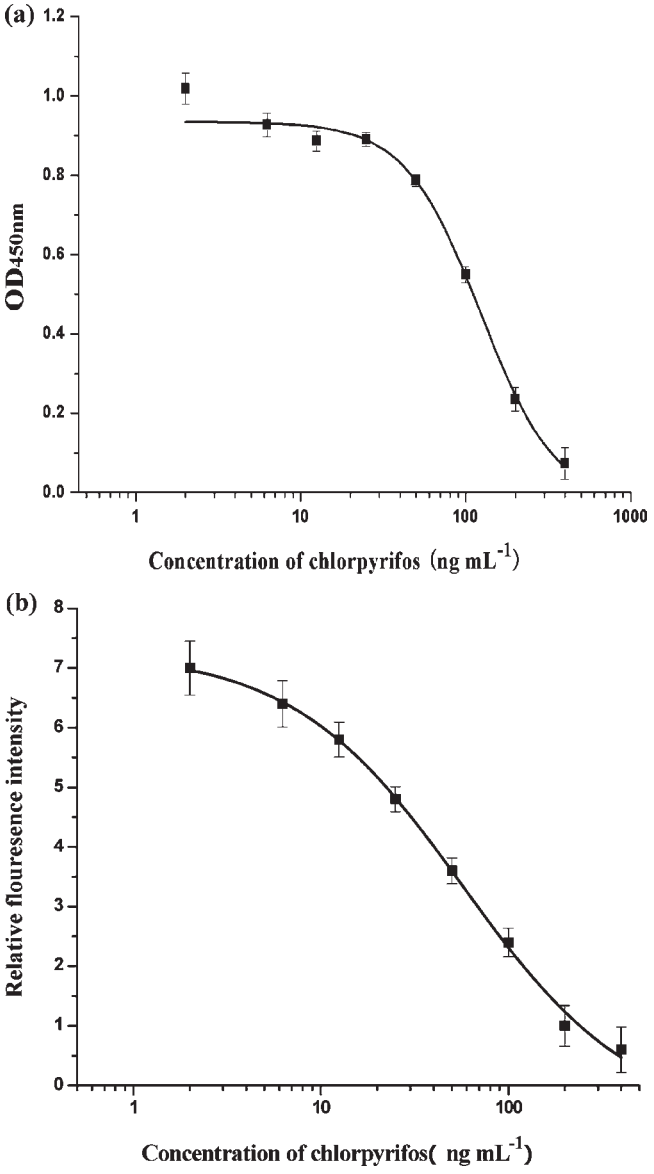

Figure 8. (**a**) Calibration curve of conventional ELISA for chlorpyrifos in PBS buffer. The sigmoid represents the standard curve of chlorpyrifos, and error bars represent the standard deviation. (**b**) Calibration curve of QDs−SA-cFLISA for chlorpyrifos in PBS. The sigmoid represents the standard curve of chlorpyrifos, and error bars represent the standard deviation.

Specificity. CR is an important parameter in evaluating the specificity of an immunoassay. The CRs of seven different chlorpyrifos structural analogues or intermediates are shown in **Table 1**. $Ab_1$was highly selective toward chlorpyrifos, and only chlorpyrifos-methyl was determined to exhibit significant cross-reactivity. Results for this study are consistent with earlier findings (*30*). The high affinity of the chlorpyrifos antibody for the methyl analogue may lead to overestimations of the target antigen. This, however, should not be problematic since chlorpyrifos-methyl is no longer registered for use in China. The CR of 3,5,6-trichloro-2-pyridinol (chlorpyrifos intermediates) suggested that the antigenic determinant was 3,5,6-trichloro-2-pyridinol. QDs−SA-cFLISA results were similar to those of conventional ELISA, indicating that the Ab_1 was very specific for chlorpyrifos.

Accuracy and Precision. Intra-assay precision was tested by conducting three replicate analyses at three concentrations ranging from 100 to 20 ng mL^{-1} in PBS buffer. The recovery was used to measure the accuracy of the assay, and the percent

Table 1. Specificity of Ab_1 to Chlorpyrifos and Its Analogues

Compound	Structure	Cross-reactivity (%) QDs-SA-cFLISA	ELISA
Chlorpyrifos	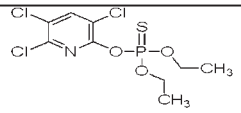	100%	100%
Chlorpyrifos-methyl	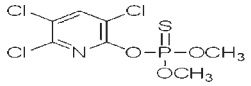	25.8%	24.5%
3,5,6-trichloro-2-pyridinol	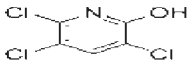	8.8%	9.2%
Fenchlor-phos	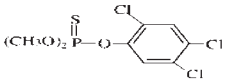	4.2%	5.3%
Bromophos	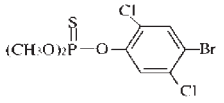	2.8%	2.5%
Parathion	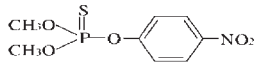	1.5%	1.8%
Triazophos	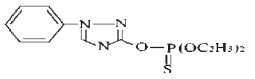	0.1%	0.2%
Chlorthion	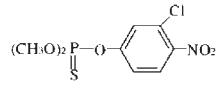	0.5%	0.4%

Table 2. Intra-Assay Reproducibility and Accuracy of QDs−SA-cFLISA and ELISA Spiked with Chlorpyrifos in PBS at Three Concentrations (n = 3)[a]

	QDs−SA-cFLISA		ELISA	
spiked (ng mL^{-1})	recovery (%)	CV (%)	recovery (%)	CV (%)
100	85.9	13.5	92.2	6.6
50	95.7	6.3	96.3	9.8
20	105.3	7.8	106.2	10.5

[a] Every spiked level was replicated three times.

coefficients of variation (CV) were used to establish the precision of antibody response at each concentration. Quality control estimations for QDs−SA-cFLISA demonstrated that it performed within a satisfactory range of variability (**Table 2**). Recoveries of 85.9% to 105.3% by QDs−SA-cFLISA and 92.2% to 106.2% by conventional ELISA were obtained at all fortification levels with CVs of 6.3% to 13.5% and 6.6% to 10.5%, respectively (**Table 2**). Recovery and CV obtained from the QDs−SA-cFLISA were similar to those from conventional ELISA. To evaluate the reproducibility of QDs−SA-cFLISA, interassay precision from three independent analyses on three different days was investigated. The mean recovery and mean CVs of all spike levels were 88.5% to 110.2% and 14.3% to 19.2%, respectively (**Table 3**). Recoveries and variabilities in the intra-assay/inter-assay satisfy current EPA criteria for the assessment of analytical methods, indicating that mean recoveries must lie within the range of 70−120%, and that CVs must lie within the range ±20%. The results shown in **Tables 2** and **3** indicate that QDs−SA-cFLISA is sufficiently accurate and can be used for further application in the detection of pesticide residues.

Matrix Effects Study. QDs−SA-cFLISA is a competitive assay format, that is, the coating antigen and the target antigen compete for antibody binding sites and are consequently prone to interference due to nonspecific binding between antibodies and nontarget analytes that may be present in a particular matrix. In addition,

Table 3. Interassay Reproducibility and Accuracy of QDs−SA-cFLISA Spiked with Chlorpyrifos in PBS and Performed on Three Separate Days

spike level (ng mL^{-1})	mean recover y(%)	mean CV (%)
100	88.5	18.5
50	92.1	15.2
20	95.6	14.3
5	110.2	19.2

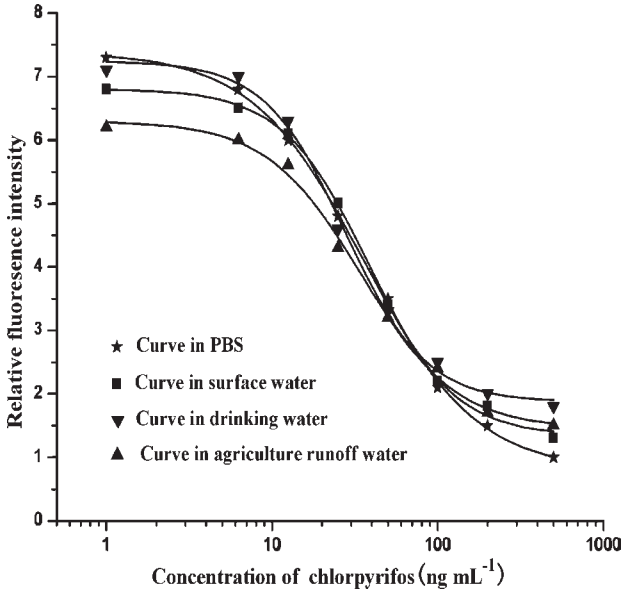

Figure 9. Analysis of matrix effect by several environmental waters (drinking water, surface water and agriculture runoff water). The result was compared with the competitive inhibition curves with standard curve in PBS.

the fluorescence signal detection system is under the matrix influence, given that fluorescence intensity of QDs is affected by the complicated matrix (**Figure 9**). Due to the fact that agricultural runoff water is rich in heavy metals (such as Cu^{2+} and Hg^{+}) and organics, it exhibits significant matrix effects, thereby affecting the fluorescent signal system. Additional resources and efforts must be directed at mitigating such influences to help degrade matrix effects. For example, the use of more aggressive preanalysis filtering techniques, centrifugation, or detergents or binding agents to reduce the amount of suspended solids and other interferences might be beneficial and should be studied more thoroughly. Overall, QDs−SA-cFLISA has practical applications in monitoring and detecting pesticide residues in food and the environment.

Drinking Water Analysis. In water sample analysis, the complex matrix effect should be minimized to attain the necessary sensitivity. In a previous section, drinking water was described as showing relatively small matrix effects in the assay, as it was diluted by PBS to degrade matrix effects. The results indicated that the matrix effect could be eliminated after a 3-fold dilution. Chlorpyrifos could not be detected in drinking water by QDs−SA-cFLISA, ELISA and HPLC method. Investigating further, serial concentrations of chlorpyrifos were added into the 3-fold diluted drinking water and the amounts of chlorpyrifos were quantified by QDs−SA-cFLISA and HPLC. There was no significant difference between the amounts of chlorpyrifos quantified by the two methods (**Table 4**). As a screening method, therefore, the detection of chlorpyrifos by the QDs−SA-cFLISA was very precise.

Comparison of Conventional ELISA and QDs−SA-cFLISA. There are many advantages in using QDs−SA-cFLISA compared with conventional ELISA (**Table 5**). First, in QDs−SA-cFLISA, a signal amplification system is applied through the

Table 4. Results from Analysis of Chlorpyrifos in Incurred Drinking Water by QDs−SA-cFLISA and HPLC (n = 3)

concn of chlorpyrifosin in drinking water (ng mL^{-1})	determined	
	QDs−SA-cFLISA	HPLC
100	102.2 ± 3.5	99.3 ± 2.7
50	51.2 ± 2.8	50.8 ± 2.5
20	20.6 ± 2.2	21.8 ± 2.0
0	ND[a]	ND

[a] ND = not determined.

Table 5. The Comparison of Conventional ELISA and QDs−SA-cFLISA Method

method	IC_{50} (ng mL^{-1})	LOD (ng mL^{-1})	working range (ng mL^{-1})	detection time (h)
ELISA	96.8	20.6	56.7−258.8	5
QDs−SA-cFLISA	28.5	3.8	10.5−180.4	4

interaction between the biotinylated Ab_1 and the QDs−SA conjugate. The utility of B−S system increases the amount of QDs linked to the biotinylated Ab_1−Ag immunocomplex, amplifying the fluorescent intensity and improving sensitivity. In addition, QDs, a fluorescent signal system in QDs−SA-cFLISA, has strong fluorescent intensity that can increase the sensitivity. Second, conventional ELISA requires labeling of antibodies with external reagents, such as enzymes and/or fluorescent dyes. This labeling procedure may cause structural changes in the epitope and suppress the specific recognition ability. Moreover, the enzymatic and fluorescence dye labeling procedures are time-consuming and may cause a high background signal. In contrast, the application of SA-coated QDs greatly simplifies the labeling procedure without affecting the binding efficiency of the Ab−Ag reaction. Third, conventional ELISA requires substrate and stop buffer reagents that are not only unstable but also harmful to human health. In comparison, QDs−SA-cFLISA can avoid this problem because QDs have long-term photostability and are very stable at RT. Finally, the detection time for QDs−SA-cFLISA is shorter by 1 h compared with conventional ELISA.

Nevertheless, there are some problems with QDs−SA-cFLISA that need further investigation, such as QDs aggregation and nonspecific absorption. QDs aggregation resulting from nonoptimal surface chemistry that, in turn, leads to the loss of colloidal stability in the biolabeling procedure is an important problem for QDs-based biosensors and immunoassay applications (*31*). In this study, the stability of the QDs−SA conjugate was directly related to the QDs/SA ratio and the pH of the reaction system, and the degree of aggregation was positively correlated with the amount of SA within a certain range. When the conjugate was dissolved in PBS−BSA solution (1% BSA, m/v), the degree of aggregation and nonspecific absorption greatly decreased. Further investigations involving adjustments in the ionic strength and species of the buffer used should be conducted to solve this problem. Moreover, it should extend the application of QDs-based immunoassays and biosensors to the analysis of pesticide residues.

Nonspecific absorption in the control group often affects the sensitivity of immunoassays. To address this concern, the PBS−BSA solution was used to minimize the background signal in our experiment. A previous research has suggested that the sizes of QD probes affect the labeling efficiency to the microsphere due to steric hindrance (*32*); the big-sized QDs probes had weaker binding capacity onto the surface of polystyrene microspheres than small-sized ones. Therefore, big-sized QDs probes can reduce nonspecific

absorption. Bruchez et al. (*33*) coated the surface of QDs with silica, and then linked biomolecules onto the silica surface. The size of these silica-coated QDs can be varied according to the objective of experiment. In further investigations, we should prepare large-sized silica-coated QDs and reduce nonspecific absorption maximally to increase the sensitivity in the optimization condition. Moreover, the labeling efficiency of QDs−SA coupling is related to the size of the QDs. Labeling efficiency may be increased by using big-sized QDs due to the big surface area.

As demonstrated in the present study, QDs−SA-cFLISA performs exceptionally well under optimal conditions, exhibiting excellent accuracy and low variability in quality control evaluations. Its overall performance characteristics in controlled assays were found to be compliant with the current U.S. EPA criteria for the assessment of analytical methods. Compared with conventional ELISA, the most significant advantage of this assay was that it increased sensitivity 5.5-fold (up to 3.8 ng mL^{-1}); thus, the sensitivity of this assay can satisfy current EPA and WHO standards for the detection of chlorpyrifos in drinking water. Therefore, QDs−SA-cFLISA could play a significant role in detecting pesticide residues, veterinary drugs residues, environment pollutants, etc.

Further studies should focus on establishing the standard procedure for labeling different Abs with QDs nanocrystals of different colors and then performing a reliable multiplexed assay by optimizing the assay conditions. It is believed that QDs nanocrystals could provide powerful fluorescent probes for the detection of pesticide residues in the future.

ABBREVIATIONS USED

Ab_1, monoclonal antibody; biotinylated-Ab_1, biotinylated monoclonal antibody; QDs−SA-cFLISA, biotin−streptavidin system competitive fluorescence-linked immunosorbent assay; BSA, bovine serum albumin; CR, cross reactivity; CV, coefficient of variation; EDC, 1-ethyl-3-(3-dimethylaminopropyl)carbodiimide; ELISA, enzyme-linked immunosorbent assay; GC−MS, gas chromatographic−mass spectrometric; HPLC, high-performance liquid chromatography; HPLC−MS, high-performance liquid chromatography−mass spectrometric; IC_{50}, 50% inhibition concentration; NHS, *N*-hydroxysulfosuccinimide sodium salt; ND, not determined; LOD, limit of detection; PBS, phosphate-buffered saline; PBST, phosphate buffered saline containing 0.05% Tween 20; QDs, quantum dots; QY, quantum yields; SEB, staphylococcal enterotoxin B; SDS−PAGE, sodium dodecyl sulfate−polyacrylamide gel electrophoresis; TNT, trinitrotoluene; TEM, transmission electron microscopy.

LITERATURE CITED

(1) Jiang, X.; Li, D.; Xu, X.; Ying, Y.; Li, Y.; Ye, Z.; Wang, J. Immunosensors for detection of pesticide residues. *Biosens Bioelectron*. **2008**, *23*, 1577–1587.

(2) Rial-Otero, R.; Gaspar, E. M.; Moura, I.; Capelo, J. L. Chromatographic-based methods for pesticide determination in honey: An overview. *Talanta* **2007**, *71*, 503–514.

(3) Núñez, O.; Moyano, E.; Galceran, M. T. LC-MS/MS analysis of organic toxics in food. *Trends Anal. Chem*. **2005**, *24*, 683–703.

(4) Bruchez, M., Jr.; Moronne, M.; Gin, P.; Weiss, S.; Alivisatos, A. P. Semiconductor nanocrystals as fluorescent biological labels. *Science* **1998**, *28*, 2013–2016.

(5) Bailey, R. E.; Smith, A. M.; Nie, S. M. Quantum dots in biology and medicine. *J. Phys. E* **2004**, *25*, 1–12.

(6) Dabbousi, B. O.; Rodriguez-Viejo, J.; Mikulec, F. V.; Heine, J. R.; Mattoussi, H.; Ober, R.; Jensen, K. J.; Bawendi, M. G. CdSe)ZnS Core-Shell Quantum Dots: Synthesis and Characterization of a Size Series of Highly Luminescent Nanocrystallites. *J. Phys. Chem. B* **1997**, *101*, 9463–9475.

(7) Sapsford, K. E.; Pons, T.; Medintz, I. L.; Mattoussi, H. Biosensing with Luminescent Semiconductor Quantum Dots. *Sensors* **2006**, *6*, 925–953.

(8) Parak, W. J.; Gerion, D.; Zanchet, D.; Woerz, A. S.; Pellegrino, T.; Micheel, C.; Williams, S. C.; Seitz, M.; Bruehl, R. E.; Bryant, Z.; Bustamante, C.; Bertozzi, C. R.; Alivisatos, A. P. Conjugation of DNA to silanized colloidal semiconductor nanocrystalline quantum dots. *Chem. Mater*. **2002**, *14*, 2113–2119.

(9) Mason, J. N.; Farmer, H.; Tomlinson, I. D.; Schwartz, J. W.; Savchenko, V.; DeFelice, L. J.; Rosenthal, S. J.; Blakely, R. D. Novel fluorescence-based approaches for the study of biogenic amine transporter localization, activity, and regulation. *J. Neurosci. Methods* **2005**, *143*, 3–25.

(10) Jin, T.; Fujii, F.; Komai, Y.; Seki, J.; Seiyama, A.; Yoshioka, Y. Preparation and Characterization of Highly Fluorescent, Glutathione-coated Near Infrared Quantum Dots for *in Vivo* Fluorescence Imaging. *Int. J. Mol. Sci*. **2008**, *9*, 2044–2061.

(11) Lingerfelt, B. M.; Mattoussi, H.; Goldman, E. R.; Mauro, J. M.; Anderson, G. P. Preparation of quantum dot-biotin conjugates and their use in immunochromatography assays. *Anal. Chem*. **2003**, *75*, 4043–4049.

(12) Goldman, E. R.; Anderson, G. P.; Tran, P. T.; Mattoussi, H.; Charles, P. T.; Mauro, J. M. Conjugation of luminescent quantum dots with antibodies using an engineered adaptor protein to provide new reagents for fluoroimmunoassays. *Anal. Chem*. **2002**, *74*, 841–847.

(13) Ding, S. Y.; Jun, X. C.; Hai, Y. J.; Ji, Y. H.; Wei, M. S.; Wen, S. Z.; Jian, Z. S. Application of Quantum Dot-Antibody Conjugates for Detection of Sulfamethazine Residue in Chicken Muscle Tissue. *J. Agric. Food Chem*. **2006**, *54*, 6139–6142.

(14) Jun, X. C.; Fei, X.; Hai, Y. J.; Ya, L. H.; Qin, X. R.; Pen, G.. G.; Shuang, Y. D. A novel quantum dot-based fluoroimmunoassay method for detection of Enrofloxacin residue in chicken muscle tissue. *Food Chem*. **2009**, *113*, 1197–1202.

(15) Jian, Z. S.; Fei, X.; Hai, Y. J.; Zhan, H. W.; Jing., T.; Peng, J. G.; Shuang, Y. D. Characterization and application of quantum dot nanocrystal−monoclonal antibody conjugates for the determination of sulfamethazine in milk by fluoroimmunoassay. *Anal. Bioanal. Chem*. **2007**, *389*, 2243–2250.

(16) Huet, A. C.; Charlier, C.; Tittlemier, S. A.; Gurmit, S.; Benrejeb, S.; Delahaut, P. Simultaneous determination of (fluoro)quinolone antibiotics in kidney, marine products, eggs, and muscle by enzyme-linked immunosorbent assay (ELISA). *J. Agric. Food Chem*. **2006**, *54*, 2822–2827.

(17) Goldman, E. R.; Medintz, I. L.; Mattoussi, H. D. Luminescent quantum dots in immunoassays. *Anal. Bioanal. Chem*. **2006**, *384*, 560–563.

(18) Moriarty, G. C.; Unabia, G. Application of the avidin-biotin-peroxidase complex (ABC) method to the light microscopic localization of pituitary hormones. *J. Histochem. Cytochem*. **1982**, *30*, 713–716.

(19) He, J. T.; Shi, Z. H.; Yan, J.; Zhao, M. P.; Guo, Z. Q.; Chang, W. B. Biotin-avidin amplified enzyme-linked immunosorbent assay for determination of isoflavone daidzein. *Talanta* **2005**, *65*, 621–626.

(20) Manclus, J. J.; Montoya, A. Development of Enzyme-Linked Immunosorbent Assays for the Insecticide Chlorpyrifos. 2. Assay Optimization and Application to Environmental Waters. *J. Agric. Food Chem*. **1996**, *44*, 4063–4070.

(21) Brun, E. M.; Garceas-Garciaa, Marta.; Puchades, Rosa.; Maquieira, Ngel. Highly sensitive Enzyme-Linked Immunosorbent Assay for chlorpyrifos. application to olive oil analysis. *J. Agric. Food Chem*. **2005**, *53*, 9352–9360.

(22) Guardino, X.; Obiols, J.; Rosell, M. G.; Farran, A.; Serra, C. Determination of chlorpyrifos in air, leaves and soil from a greenhouse by gas-chromatography with nitrogen−phosphorus detection, high-performance liquid chromatography and capillary electrophoresis. *J. Chromatogr., A* **1998**, *823*, 91–96.

(23) Zhang, H..; Yang, B. X-Ray Photoelectron Spectroscopy Studies of the Surface Composition of Highly Luminescent CdTe Nanoparticles in Multilayer. *Thin Solid Films* **2002**, *418*, 169–174.

(24) Zhelev, Z.; Bakalova, R.; Ohba, H.; Jose, R.; Imai, Y.; Baba, Y. Versatile Immunosensor Using CdTe Quantum Dots as Electrochemical and Fluorescent Labels. *Anal. Chem*. **2006**, *78*, 321–330.

(25) Zhang, B. B.; Gong, X. Q.; Hao, L. J.; Cheng, J.; Han, Y.; Chang, J. A novel method to enhance quantum yield of silica-coated quantum dots for biodetection. *Nanotechnology* **2008**, *19*, 1–9.
(26) Zhelev, Z.; Ohba, H.; Bakalova, R.; Jose, R.; Fukuoka, S.; Nagase, T.; Ishikawa, M.; Baba, Y. Fabrication of quantum dot-lectin conjugates as novel fluorescent probes for microscopic and flow cytometric identification of leukemia cells from normal lymphocytes. *Chem. Commun.* **2005**, *15*, 1980–1982.
(27) Manclús, J. J.; Primo, J.; Montoya, A. Development of an enzyme-linked immunosorbent assay for the insecticide chlorpyrifos. 1. Monoclonal antibody production and immunoassay design. *J. Agric. Food Chem.* **1996**, *44*, 4052–4062.
(28) Goldman, E. R.; Anderson, G. P.; Tran, P. T.; Mattoussi, H.; Charles, P. T.; Mauro, J. M. Conjugation of luminescent quantum dots with antibodies using an engineered adaptor protein to provide new reagents for fluoroimmunoassays. *Anal. Chem.* **2002**, *74*, 841–847.
(29) Zhang, F.; Li, C.; Li, X.; Wang, X.; Wan, Q.; Xian, Y.; Jin, L.; Yamamoto, K. ZnS quantum dots derived a reagentless uric acid biosensor. *Talanta* **2006**, *68*, 1353–1358.
(30) Jonathan, J. S.; Ye, G. C.; Kean, S. G. Performance Assessment and Validation of a Paramagnetic Particle-Based Enzyme-Linked Immunosorbent Assay for Chlorpyrifos in Agricultural Runoff Waters. *J. Agric. Food Chem.* **2007**, *55*, 6407–6416.
(31) Seydack, M. Nanoparticle labels in immunosensing using optical detection methods. *Biosens. Bioelectron.* **2005**, *20*, 2454–2469.
(32) Bailey, E. R.; Smith, A. M.; Nie, S. Quantum dots in biology and medicine. *Physica E* **2004**, *25*, 1–12.
(33) Bruchez, M.; Moronne, M.; Gin, P.; Weiss, S.; Alivisatos, A. P. Semiconductor nanocrystals as fluorescent biological labels. *Science* **1998**, *281*, 2013–2016.

Received for review February 3, 2010. Revised manuscript received July 12, 2010. Accepted July 12, 2010. The authors gratefully acknowledge the financial support by National High Technology R&D Program of China (No. 2007AA06Z419), Natural Science Foundation of China (No. 30771810) and Science and Technology Program of Tianjin (No. 09ZCKFSH02700).